An Experimental and Mathematical Study on the Effects of Ignition Energy and System on the Flame Kernel Development

Jeonghoon Song*

Department of Mechanical Engineering, Inje University,
607 Obang~dong, Kimhae, Kyungnam 621~749, Korea

Myoungho Sunwoo

Department of Automotive Engineering Hanyang University,
17 Haengdang-dong, Sungdong-ku, Seoul 133~791, Korea

A constant volume combustion chamber is used to investigate the flame kernel development of gasoline air mixtures under various ignition systems, ignition energies and spark plugs. Three kinds of ignition systems are designed and assembled, and the ignition energy is controlled by the variation of the dwell time. Several kinds of spark plugs are also tested. The velocity of flame propagation is measured by a laser deflection method, and the combustion pressure is analyzed by the heat release rate and the mass fraction burnt. The results represent that as the ignition energy is increased by enlarging either dwell time or spark plug gap, the heat release rate and the mass fraction burnt are increased. The electrodes materials and shapes influence the flame kernel development by changing he transfer cfficiency of electrical energy to chemical energy. The diameter of electrodes also influences the heat release rate and the burnt mass fraction.

Key Words : Heat Release Rate, Burnt Mass Fraction, Ignition System, Spark Plug

Nomenclature

p : Pressure
v : Volume per unit mass
q : Chemical energy per unit mass
q_{loss} : Energy losses per unit mass
c_v : Coefficient of constant volume

Greek letters

$\varnothing$: Equivalence ratio

Subscripts

a : Air
f : Fuel
ini : Initial
max : Maximum

* Corresponding Author,
 E-mail : mechsong@ijnc.inje.ac.kr
 TEL : +82-55-320-3755; **FAX :** +82-55-324-1723
 Department of Mechanical Engineering, Inje University,
 607 Obang-dong, Kimhae, Kyungnam 621-749, Korea.
 (Manuscript **Received** July 23, 2001; **Revised** March 4, 2002)

1. Introduction

With declining oil reserves and increasing fuel costs, it is imperative that motor vehicle engines operate with improved thermal efficiency. It is well known that higher engine efficiencies are obtained by operating at a high compression ratio and by burning lean mixtures. The latter is also of benefit for reducing the level of exhaust emissions. In order to burn lean mixtures effectively, it is necessary to accelerate combustion and compensate for the lower burning velocity of weak mixtures. Farthermore, Fast burning is also required in order to avoid the onset of knocking at high compression ratios. It has clearly been demonstrated that accelerated burning rates can be achieved by adopting high ignition energies or by optimal designs of spark plug.

Dulger et al. (1994) and Kravchik et al. (1995) described the ignition process, modeled the development of initial flame kernel and simulated

the effect of spark plug configurations. Daniels and Scilzo (1996) performed experimental studies with several spark plugs in spark ignition engines. Arcoumanis and Bae (1992) measured the inducted mixture flow in a constant volume combustion chamber and ignition energy, analyzing the burnt mass fraction and flame development velocity. They also changed the kinds of spark plugs, and visualized the flame propagation. Fujimoto et al. (1995) used a pancake-type constant-volume combustion chamber to investigate the combustion, and NOx emission characteristics of propane-air and hydrogen-air mixtures under various charge stratification patterns.

Most of these researches analyzed the initial flame developments that include the effect of mixture flow or stratified mixture distribution. Therefore, these experimental conditions contain the turbulence effects, and it is difficult to identify clearly the influences of ignition system or ignition energy on the flame development.

Thus, this study attempts to remove the effect of turbulence flame by using the constant volume combustion chamber (CVCC). Specifically, in order to reduce the gas flow and to make a homogenous mixture, the mixture is ignited three minutes after the mixture is inducted into the chamber.

In addition, several kinds of ignition systems and spark plugs are designed and evaluated. The characteristics of flame propagation are analyzed by the laser deflection method and by the combustion pressure. The heat release rate and mass fraction burnt are calculated by the measured pressure.

2. Experimental Systems and Procedure

Figure 1 represents a schematic diagram of the experimental system, and Fig. 2 shows the dimensions of the constant volume combustion chamber.

The air compressor supplies the air to the premixer, and the fuel injection system regulates the amount of injected fuel according to the predetermined air-fuel ratio. The inducted air
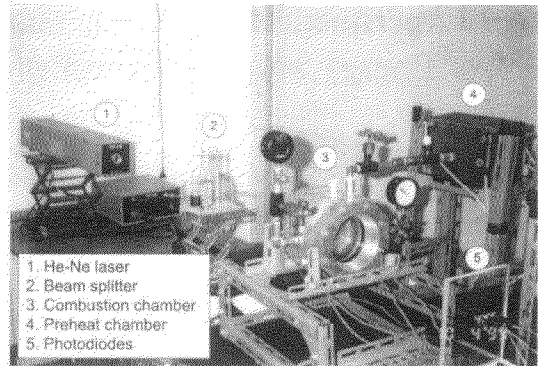

1. He-Ne laser
2. Beam splitter
3. Combustion chamber
4. Preheat chamber
5. Photodiodes

Fig. 1 Experimental system apparatus
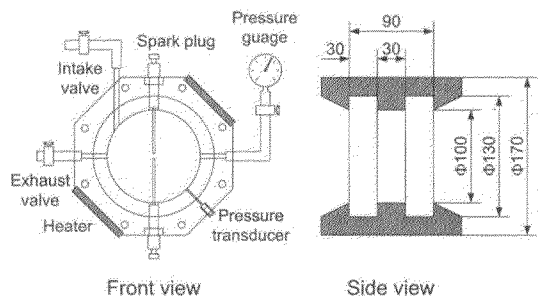

Front view   Side view

Fig. 2 Schematic diagram of constant volume combustion chamber

and fuel are mixed and stay for three minutes to completely vaporize. Well-mixed gas in the premixer is inducted into the combustion chamber and combusted. At last, the flame propagation velocity and combustion pressure are measured. The acquired data are amplified, A/D converted and then input to a data acquisition system. The dwell time and ignition time are controlled by the spark timing controller.

2.1 Experimental systems

2.1.1 Constant volume combustion chamber (CVCC)

The constant volume combustion chamber is composed of the premixer and the combustion chamber.

The premixer is designed to control the air/fuel ratio and to vaporize the injected fuel. It is made of brass to heat quickly and installed 400W and 600W heaters at both side. The volume of the premixer is $2650 \times 10^{-6} \mathrm{m}^3$.

The combustion chamber is made of dur-alumin, and the windows of both sides are made of quartz to visualize the flame (Fig. 2). The electrodes gap is located at the center of the chamber for the sake of conveniently inspecting the development of initial flame kernel. The pressure and temperature of the premixer and the combustion chamber is maintained at 6bar and at 120°C, respectively.

2.1.2 Ignition systems

Three kinds of IDI (Inductive Discharge Ignition) systems are designed and manufactured. One of them is a DIS (Direct Ignition System), which is a conventional ignition system widely used in commercial cars and has two spark plugs per ignition coil. The next one is named HEI (High Energy Ignition) system, which is modified from the DIS to intensify the ignition energy. HEI has two spark plugs equipped with two ignition coils instead of one ignition coil. The third one is an I-DIS (IGBT-based Direct Ignition System) which uses an IGBT (Insulated Gate Bipolar Transistor) for driving the ignition coil instead of using BJT (Bipolar Junction Transistor) which is adopted by most conventional DIS's.

The IGBT (Insulated Gate Bipolar Transistor) is known for fast switching performance, small on-state loss and switching loss, and ease of driving, because it is a voltage-controlled device compared to the BJT (Mohan et al., 1995). More specific circuit diagrams of the ignition systems tested in this study are represented in the research result of Song et al. (1999).

Table 1 Conditions of experimental tests

Ignition system	DIS, HEI, I-DIS
Dwell time	1.5, 2.5, 3.5 msec
Electrode gap	0.8, 1.2, 2.0mm
Electrode material	copper, nickel, tungsten
Electrode diameter	1.2, 2.0, 2.8mm
Electrode shapes	sharp, flat
Electrode ratio	0.8, 1.0
Fuel	gasoline

2.1.3 Spark plugs

Several different configurations of spark plugs are also employed to analyze the effects of the electrode on the flame kernel formation and development, such as the gap, material, diameter and shape of the electrodes. Table 1 represents the experimental conditions which are kinds of spark plugs and ignition systems, variations of dwell times and air-fuel ratios.

2.2 Experimental Procedure

The current and voltage are measured about 200 times for all experimental conditions with current probe (Tektronix A6303) and voltage probe (Tektronix P6015). The ignition energies are calculated with these values. The combustion pressure and flame propagation are measured simultaneously at least 30 times for all conditions.

2.2.1 Air-fuel ratio control

In order to control the air/fuel ratio, the premixer is employed, and the amount of injected gasoline is regulated with the following equations. The mass of inducted air is calculated with ideal gas law as follow,

$$m_a = \frac{pV}{R_a T}$$
$$= \frac{p(\text{bar}) \times 10^5 \times 265 \times 10^{-5} \times 1000}{0.287 \times 10^3 \times (T(°C) + 273)}(g) \quad (1)$$

The gas constant of air, R_a, is assumed as 0.287(J/kg/K), and the volume of premixer is $265 \times 10^{-5} \text{m}^3$.

The amount of injected fuel is calculated from the definition of equivalence ratio. The equivalence ratio is defined as the actual fuel/air ratio divided by the stoichiometric fuel/air ratio.

$$\Phi = \frac{(m_f/m_a)_{act}}{(m_f/m_a)_{stoichiometric}} = \frac{(m_f/m_a)}{14.7^{-1}}$$
$$= \frac{m_f/m_a}{6.803 \times 10^{-2}} \quad (2)$$

Thus, the amount of gasoline for each equivalence ratio is determined by

$$m_f = \Phi \times m_a \times 6.803 \times 10^{-2}$$
$$= \Phi \times \frac{p \times 922.7}{(T+273)} \times 6.803 \times 10^{-2} \quad (3)$$

With an electrical scale (Ohaus Co., TP200S), the gasoline is measured, and by controlling the injector pulse, the proper quantity of gasoline is injected.

2.2.2 Measurement of flame propagation

The flame development velocity is measured by the laser deflection method. Fig. 3 represents the schematic of the experimental apparatus.

The output laser beam from the He-Ne laser (50mW, 632. 5mm) is divided into three parallel beams by beam splitters. The split beams pass through the combustion chamber, and are then imaged onto three photodiodes. When the flame intersects a beam, the refractive index gradients present locally deflect the beams off the photodiode, which indicate the arrival time of the flame
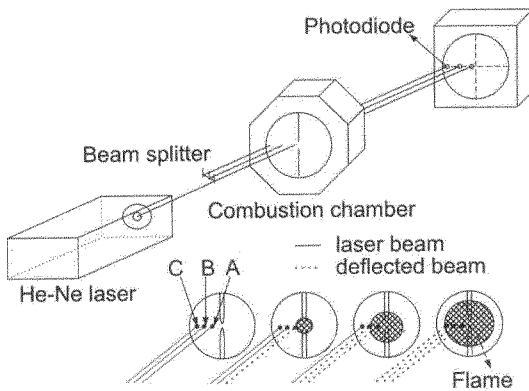

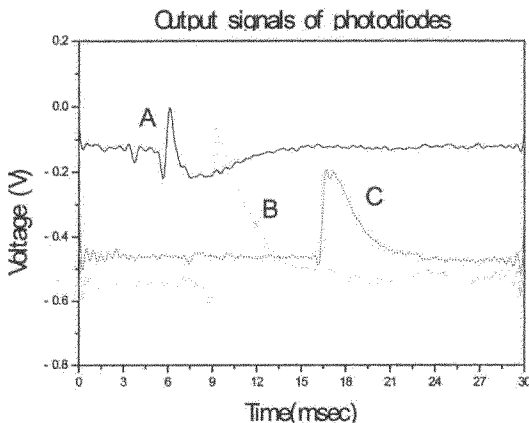**Fig. 3** Configuration of the laser deflection method

Fig. 4 Filtered output signals of photodiodes

at the measurement location. The measurement positions are located at 5mm (A point), 10mm (B), and 20mm (C) from the spark plug gap, respectively, as shown in Fig. 3. The velocity at location A represents the initial flame growth.

Figure 4 shows an example of the filtered output signals from the photodiodes. It is assumed that the highest value of each signal expresses the arrival time of the flame at each measurement location.

2.2.3 Measurement of pressure development

The combustion pressure at the CCVC is exclusive of pressure rise by turbulence flame due to reduction of mixture flow and homogeneous mixture distribution. Therefore, it contains more definite information about the influences of ignition systems and discharged energy. The pressure is measured with a piezo-electric type pressure sensor (Kistler, 6121).

Although there are a lot of approaches that analyze the combustion pressure, in this research, the heat release rate and the mass fraction burnt are adopted. These two methods are based on the reciprocal assumption. The heat release rate assumes that the pressure variation is related to the chemical energy released by combustion rather than to the burnt mass of mixture, and the mass fraction burnt analysis assumes the pressure variation is closely related to the mass of burnt mixture (Fujimoto et al., 1995; Heywood, 1988).

• **Heat release rate** (dq/dt) A major advantage of the heat release rate approach is the simplicity of treating the combustion chamber contents as a single zone, and ease of calculation with the first law of thermodynamics (Heywood, 1988; Song et al., 2000).

Based upon the first law of thermodynamics, this study derives the heat release rate as follows:

$$\delta q = c_v dT + \delta q_{loss} \qquad (4)$$

From the ideal gas law,

$$\frac{dp}{p} + \frac{dv}{v} = \frac{dT}{T} \qquad (5)$$

Substituting the first term on the right side of Eq. (4) with Eq. (5), and differentiating the rearranged equation with respect to time, the heat
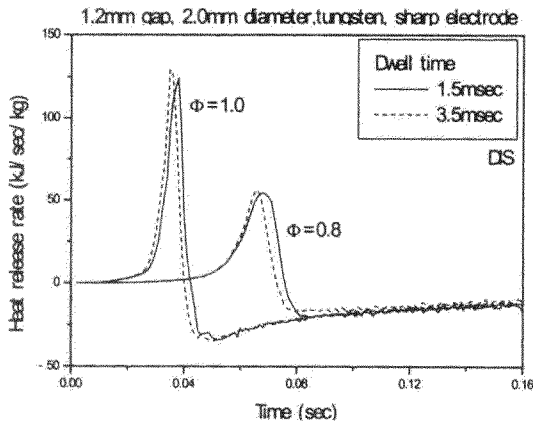
1.2mm gap, 2.0mm diameter,tungsten, sharp electrode

Fig. 5 An example of heat release rate variation caused by dwell time change (Condition : 6bar, 150°C)

release rate is obtained as follows,

$$\dot{q} = v \frac{c_v}{R} \frac{dp}{dt} + \dot{q}_{loss} \qquad (6)$$

The calculation results are analyzed by two parameters, h_{max} and h_{max_t}. h_{max} represents the value of maximum heat release rate, and h_{max_t} is the time period from the start of ignition to the time that the maximum heat release rate occurs. Figure 5 shows an example of the analysis of heat release.

• **Burnt mass fraction** The burnt mass fraction is calculated from the measured pressure trace based on the assumption that combustion pressure corresponds to the fraction as shown in Fig. 6 and calculated by Eq. (7) (Fujimoto et al., 1995; Song and Sunwoo, 2000)

$$M(t) = \frac{p(t) - p_{ini}}{p_{max} - p_{ini}} \qquad (7)$$

The flame kernel development duration, t_{0-10}, is defined as the time period from the ignition to the time at which 10% burnt mass fraction occurs, and the flame propagation duration, t_{10-90}, is also defined as the time period during which the burnt mass fraction changes from 10 to 90%. The nomenclature, t_{max}, is the duration from the ignition to the time that all the mixture in the combustion chamber is burnt.
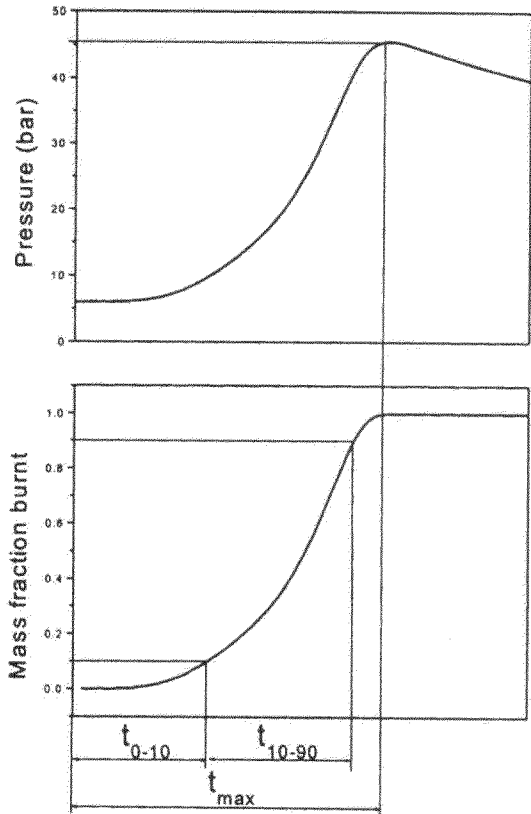

Fig. 6 Definition of burnt mass fraction and combustion duration (t_{0-10}, t_{10-90} and t_{max}) and corresponding pressure transition

3. Experimental Results

In order to represent the experimental results, this study adopts the velocities (velocity at location A, B and C), heat release rate (h_{max} and h_{max_t}), and mass fraction burnt (t_{0-10}, t_{10-90}, and t_{max}). The ignition energy is also measured at each driving condition.

3.1 Dwell time

The dwell time means that the duration of the primary circuit of the ignition system is the electrically on state and stores ignition energy at ignition a coil(s) and/or a capacitor(s).

As the dwell time is increased, the stored ignition energy is also increased until it is saturated. The result suggests that when the dwell time is extended from 1.5msec to 3.5msec, the ignition energies of the DIS, HEI, and I-DIS at 3msec

Table 2 Effects of dwell times on flame kernel development at $\Phi=0.8$

	dwell (msec)	energy (mJ)	A (m/sec)	B (m/sec)	C (m/sec)	h_{max} (J/sec/g)	h_{max_t} (msec)	t_{0-10} (msec)	t_{10_90} (msec)	t_{max} (msec)
DIS	1.5	9.6	1.081	1.006	0.978	54.5	68	32	33	72
	3.5	15.8	1.142	1.059	1.026	56.4	66	30	32	69
HEI	1.5	17.6	1.148	1.067	1.039	57.6	66	28	34	68
	3.5	29.1	1.203	1.092	1.077	59.4	64	26	33	66
I-DIS	1.5	10.4	1.102	1.037	1.998	54.5	67	31	33	72
	3.5	22.1	1.183	1.109	1.074	58.6	64	28	33	68
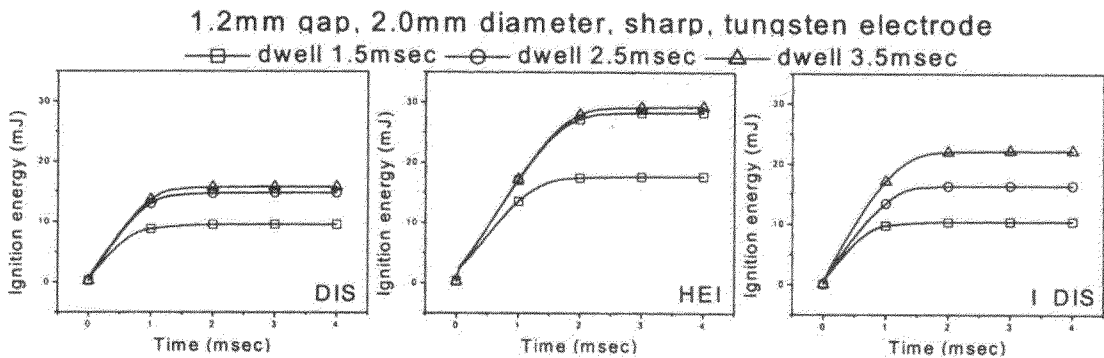
Fig. 7 Effects of dwell time on ignition energy for three ignition systems (Condition : 6bar, 150°C)

after the ignition occurs increases by about 65%, 60%, and 113%, respectively.

However, Fig. 7 reflects that the DIS and HEI are saturated when the dwell time is extended around 3msec. When saturation occurs, despite extended dwell time, the total stored energy will not be changed.

Table 2 explains the influences of the dwell time on the characteristics of flame kernel development. As the dwell time is extended from 1.5msec to 3.5msec, the initial flame propagation velocity which is measured and calculated at position A, is increased by about $5\sim7\%$, and t_{0-10} is reduced by about $7\sim11\%$ for all three ignition systems. However, t_{10-90} is not affected by dwell time. This means that the ignition system and ignition energy seldom exert influence on flame propagation except initial flame kernel development. The heat release rate is also affected by dwell time, as shown in Table 2.

3.2 Spark plug gap
Table 3 represents the effects of the spark plug

gap on ignition energy. The discharged energy of the DIS with a gap width of 2.0mm rises by about 74% in companison with a gap width of 0. 8mm. For the HEI, the ignition energy is increased by about 68% while the I-DIS records an increase of about 109%. These increases in ignition energy with a widened spark gap can be attributed to the extended surface of the plasma, which requires more energy to sustain itself, particularly in conditions where the energy density is held constant, resulting in a constant temperature gradient along the plasma surface (Arcoumanis and Bae, 1992).

Table 3 also explains the flame growth velocity, mass fraction burnt and heat release rate at $\Phi=0.8$. When the gap is increased from 0.8mm to 2.0mm, the velocities at location A are increased by about $7\sim8$cm/sec from $1.121\sim1.188$m/sec and the initial 10% mass fraction burnt is hastened by about $4\sim5$msec from $28\sim32$msec with three ignition systems. These results come from the increased ignition energy and the expanded plasma volume which contacts unburned gas.

Table 3 Effects of spark plug gaps on flame kernel development at $\Phi=0.8$

	gap (mm)	energy (mJ)	A (m/sec)	B (m/sec)	C (m/sec)	h_{max} (J/sec/g)	h_{max_t} (msec)	t_{0-10} (msec)	t_{10_90} (msec)	t_{max} (msec)
	0.8	11.8	1.121	1.042	1.007	54.6	68	32	33	72
DIS	1.2	15.8	1.142	1.059	1.026	56.4	66	30	32	69
	2.0	20.5	1.198	1.105	1.052	57.2	61	28	33	67
	0.8	20.3	1.188	1.091	1.054	57.3	66	28	33	68
HEI	1.2	29.1	1.203	1.092	1.007	59.4	64	26	33	66
	2.0	39.4	1.253	1.133	1.104	61.8	60	24	33	64
	0.8	15.7	1.142	1.06	1.031	56.9	66	30	33	70
I-DIS	1.2	22.1	1.183	1.109	1.074	58.6	64	28	33	68
	2.0	32.8	1.223	1.142	1.088	61.1	62	25	33	66

Table 4 Effects of electrode Materials on flame kernel development at $\Phi=0.8$

	mat.	energy (mJ)	A (m/sec)	B (m/sec)	C (m/sec)	h_{max} (J/sec/g)	h_{max_t} (msec)	t_{0-10} (msec)	t_{10_90} (msec)	t_{max} (msec)
	Cu	17.3	1.177	1.083	1.057	60.3	61	28	33	68
DIS	Ni	16.3	1.16	1.078	1.039	59.8	63	29	33	68
	W	15.8	1.142	1.059	1.26	56.6	66	30	32	69
	Cu	31.1	1.232	1.144	1.102	64.7	59	25	32	65
HEI	Ni	29.7	1.213	1.118	1.087	62.1	61	25	33	65
	W	29.1	1.203	1.092	1.077	59.4	64	26	33	66

As a result of faster kernel development, the maximum heat release rate is increased. The maximum heat release rates of DIS, HEI and I-DIS are increased by 2.6, 4.5, and 4.2kJ/sec/kg from 54.6, 57.3, and 56.9kJ/sec/kg, respectively.

3.3 Electrode materials

This experiment is done to research the effects of electrode materials on ignition energy and expansion velocity of the flame kernel. Table 4 represents the experimental results. The materials of electrodes used in this research are copper, nickel, and tungsten. The melting temperatures of copper, and tungsten are 3660K. The results show, when the melting temperature of an electrode is higher, the ignition energy is decreased about 7~9%. Table 4 also explains the heat release rate and burnt mass fraction.

As the melting temperature of electrodes is lowered, the transfer efficiency of discharge energy is raised. Since the lower melting temperature

material liberates electrons easier, the current density becomes higher (Ziegler et al., 1984). When the current grows, the discharge phase is transferred from glow to arc phase. As a consequence of that the energy transfer efficiency is increased from 30% to 50%. This accelerates the flame propagation velocity.

3.4 Electrode diameters

The heat losses to the electrode vary the flame propagation velocity, which is affected by electrode materials, electrode diameters and so on (Lim et al., 1987, Ko et al., 1991).

Table 5 represents the variation of flame propagation when the electrode diameters are changed. From this experiment, it is noticed that the discharged energy and flame propagation velocity are not affected as much as when the parameters such as dwell time, electrode gap and material are varied.

However, there is a tendency that as the diame-

Table 5   Effects of electrode diameters on flame kernel development at $\Phi=0.8$

|	dia. (mm)	energy (mJ)	A (m/sec)	B (m/sec)	C (m/sec)	h_{max} (J/sec/g)	h_{max_t} (msec)	t_{0-10} (msec)	t_{10_90} (msec)	t_{max} (msec)
	1.2	16.7	1.163	1.077	1.046	60.3	64	29	32	68
DIS	2.0	15.8	1.142	1.059	1.026	56.4	66	30	32	69
	2.8	15.1	1.128	1.056	1.011	55.3	67	31	33	70
	1.2	30.8	1.224	1.123	1.069	62.8	62	25	33	66
HEI	2.0	29.1	1.203	1.092	1.077	59.4	64	26	33	66
	2.8	27.1	1.189	1.078	1.061	57.4	65	26	34	68

Table 6   Effects of electrods shapes on flame kernel development at $\Phi=0.8$

	mat.	energy (mJ)	A (m/sec)	B (m/sec)	C (m/sec)	h_{max} (J/sec/g)	h_{max_t} (msec)	t_{0-10} (msec)	t_{10_90} (msec)	t_{max} (msec)
DIS	flat	14.8	1.105	1.025	1.001	52.9	68	31	34	72
	sharp	15.8	1.142	1.059	1.026	56.4	66	30	32	69
HEI	flat	26.7	1.172	1.081	1.05	54.9	65	27	33	68
	sharp	29.1	1.203	1.092	1.077	59.4	64	26	33	66

ter of an electrode is reduced, the ignition energy is increased. This result shows that when the electrode diameter is reduced from 2.8mm to 1.2mm, then the ignition energy is raised by about $11\sim14\%$. The flame velocity at location A accelerates by about 3% for both ignition systems, and t0-10 is reduced by about 7% for the DIS, and 4% for the HEI.

3.5 Electrode shapes

As shown in Fig. 8, the electrode shapes are changed for test purpose. The variation of the electrode shape affects flame propagation due to the change of the discharge phase. If the number of emitted electrons from the electrode is the same, the smaller or sharper tip of the electrode increases the density of the discharged current, which changes the ignition phase from glow to arc phase which, in turn, causes the higher energy transfer efficiency (Pischinger and Heywood, 1990). As a result, the propagation velocities at location A with the DIS and the HEI are increased to 3.5cm/sec and 3.1cm/sec from 1.107 m/sec and 1.172m/sec, respectively, in the case of $\Phi=0.8$. The heat release rate and the burnt mass fraction also increase, as represented in Table 6.
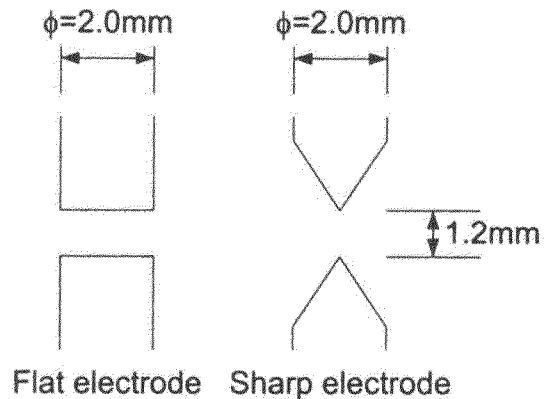
Fig. 8   Shape of electrodes

4. Conclusion

A constant volume combustion chamber is used to investigate the flame kernel growth and flame propagation of the gasoline-air mixture under various ignition systems and spark plugs. A laser deflection method is applied to measure the flame propagation velocity, and a piezo-electronic type pressure sensor is used to evaluate the combustion pressure. The heat release rate and burnt mass fraction are calculated from the measured pressure data.

The major findings from this research are as follows:

(1) As the dwell time is increased from 1.5msec to 3.5msec, the discharged energy is also increased by about 40~113%. All ignition systems evaluated in this research (DIS, HEI, and I-DIS), accelerate growth of the initial flame kernel by 5.5~8.1cm/sec from 1.081~1.148 m/sec, and reduce the initial flame growth period by 2~3msec from 28~32msec as the dwell time is increased. However, the flame propagation period is affected by neither the ignition system nor the discharged energy. The duration from ignition to the maximum heat release rates are shortened by 2~3msec from the 66~68msec, and the maximum heat release rate is raised by 1.8~3.1kJ/sec/kg from 55~58kJ/sec/kg with all ignition systems. However, when the dwell time of the DIS and HEI are increased more than 3msec, the stored ignition energy is saturated, and thus, the ignition energy is not changed.

(2) When the spark plug gap is extended from 0.8mm to 2.0mm, the discharged energy is increased by 74~110% in the three ignition systems. As the gap is extended, the volume of plasma is also increased, and to sustain the expanded plasma, increased ignition energy is required. The increased plasma can enlarge the contact area with unburned gas, and it stimulates the growth of the initial kernel. As a results, the first 10% of burnt mass fraction is reduced by about 14~20%.

(3) The material of the electrode affects the ignition energy and flame propagation, which is closely related with its melting temperature. The spark plug with a lower melting temperature electrode yields higher ignition energy and higher transfer efficiency. The spark plug of copper electrode discharges 7~16% more energy than that of the tungsten electrode and the initial flame growth period, t_{0-10}, is also decreased by about 4~7% with the DIS and the HEI.

(4) The diameter of electrode also influences the discharged energy and growth of flame kernel. As the diameter is reduced from 2.8mm to 1.2mm, the discharged energies of the DIS and HEI are elevated about 9~14%. Consequently, the initial flame development velocity is enhanced and the time of maximum heat release rate is also hastened for both DIS and HEI.

(5) As the electrodes tip is sharpened, the discharged energy is increased, and the current density is raised. When the current density is raised, the transfer efficiency is increased so that it helps the growth of the initial flame kernel. When sharp electrodes are used, the discharged energies of DIS and HEI are increased by 7% and 9%, respectively.

References

Arcoumanis, C. and Bae, C., 1992, "Correlation between Spark Ignition Characteristics and Flame Development in a Constant-Volume Combustion Chamber," *SAE Transaction*, SAE paper 920413.

Daniels, C. F. and Scilzo, B. M., 1996, "The Effects of Electrode Design on Mixture Ignitability," *SAE Transaction*, SAE paper 960606.

Dulger, M., Sher, E. and Chemla, F., 1994, "Simulation of Spark Created Turbulent Flame Development Through Numerical Stochastic Realization," *Combustion Science and Technology*, Vol. 100, pp. 141~162.

Fujimoto, M., Nishida, K. Hyroyasu, H. and Tabata, M., 1995, "Influence of Mixture Stratification Pattern on Combustion Characteristics in a Constant-Volume Combustion Chamber," *SAE Transaction*, SAE paper 952412.

Heywood, J. B., 1988, *Internal Combustion Engine Fundamentals*, McGraw-Hill. Chap 9., pp. 371~490.

Ko, Y., Anderson, R. W., and Arpaci, V. S., 1991, "Spark Ignition of Propane-Air Mixture Near the Minimum Ignition Energy," Combustion and Flame, Vol. 83, pp. 75~87.

Krabchik, T., Sher, E. and Heywood, J. B., 1995, "From Spark Ignition to Flame Initiation," *Combustion Science and Technology*, Vol. 108, pp. 1~30.

Lim, M. T., Anderson, R. W. and Arpaci, V. S., 1987, "Prediction of Spark Kernel Development in Constant Volume Combustion," Combustion and Flame, Vol. 69, pp. 303~316.

Mohan, N., Undeland, T., and Kobbins, W., 1995, Power Electronics, Willy & Sons. Chap. 26, pp. 626~640.

Pischinger, S. and Heywood J. B., 1990, "How Heat Losses to the Spark Plug Electrodes Affect Flame Kernel Development in an SI Engine," *SAE Transaction*, SAE paper 900021.

Song, J., Sunwoo, M. and Kim, W., 1999, "A Study on the Engine Performance Improvement of a Lean Burn Engine by High Energy Ignition," *Transaction of Korea Society of Automotive Engineers*, Vol. 7, No. 2., pp. 31~40.

Song, J., Sunwoo, M., 2000, "A Visualization Study on the Effects of Ignition Systems on the Flame Propagation in a Constant Volume Combustion Chamber", *Journal of KSME (B)*, Vol. 24, No. 12, pp. 1652~1661.

Song, J., Lee, K. and Sunwoo, M., 2000, "A Study on the Effects of Ignition Systems on the Heat Release Rate and Mass Fraction Burnt at a Constant Volume Combustion Chamber," *Journal of KSME (B)*, Vol. 24, No. 11, pp. 1486~1496.

Ziegler, G., Wagner, E. and Maly, R., 1984, "Ignition of Lean Methane-Air Mixtures by High Pressure Glow and Arc Discharges," *20th Symposium (International) on Combustion*, Combustion Institute.